JOURNAL OF CATALYSIS 157, 109–123 (1995)

Crystal Phase, Spectral Features, and Catalytic Activity of Sulfate-Doped Zirconia Systems

C. Morterra,* G. Cerrato,* F. Pinna,† and M. Signoretto†

*Department of Inorganic, Physical, and Materials Chemistry, University of Turin, Via P. Giuria 7, I-10125 Turin, Italy; and †Department of Chemistry, University of Venice, Calle Larga St. Marta 2137, I-30123 Venice, Italy

Received December 20, 1994; revised April 18, 1995; accepted June 12, 1995

Several sulfate-doped ZrO_2 catalysts (s.d.-ZrO_2) have been prepared by sulfating, with either sulfuric acid or ammonium sulfate, samples of monoclinic ZrO_2, Y_2O_3-stabilized tetragonal ZrO_2, and amorphous Zr hydroxide, and by calcining the sulfated precursors at $T \geq 673$ K. We then examined (by TEM, XRD, FTIR, and catalytic tests) the effect of sulfation on ZrO_2 crystal phase and morphology, the effect of ZrO_2 crystal phase on the spectroscopic features of the surface sulfate groups, and the catalytic behaviour of the three families of s.d.-ZrO_2 systems in the isomerization of *n*-butane. It could be concluded that the sulfated monoclinic ZrO_2 phase is catalytically not very active (if at all), the nonstabilized tetragonal ZrO_2 phase is unstable to the sulfation process, and the sulfated tetragonal ZrO_2 phase is catalytically active, no matter what the preparative route has been, provided that the sulfated system is calcined at $T \geq 823$ K. The latter condition is discussed in terms of the structural and spectroscopic features of the surface sulfate layer.

INTRODUCTION

Hino *et al.* (1) first reported that zirconium oxide, modified at the surface with sulfates, may develop unusually strong acidic properties and unique catalytic activity. For these sulfate-doped zirconias (s.d.-ZrO_2), the definition of solid superacid has been used (2), although not all the authors admit that the behaviour of s.d.-ZrO_2, based on the determination of Hammett's H_0 acidity function, is really that of a superacid solid (3).

As already suggested by Arata (4), we are convinced that the most suitable way to check if a catalytic system (s.d.-ZrO_2 or otherwise) actually did acquire the features that ought to be thought of as peculiar of a superacid system is to test the system with some catalytic reactions typical of superacid catalysis (like, for instance, the low-temperature isomerisation of *n*-alkanes). In the present contribution, the isomerisation of *n*-butane at 423 K will be adopted as a standard test to assess the superacid catalytic properties of various families of s.d.-ZrO_2 systems.

In recent years it has been shown that the acidic and catalytic properties of s.d.-ZrO_2 catalysts depend on a very high number of preparative parameters (4–6), among which sulfation procedure, sulfate content, concentration of the sulfating agent, and catalyst activation temperature seem to be quite important.

As far as the sulfation procedure is concerned, several authors have suggested that:

(i) the chemical nature of the sulfating agent and the sulfation process are not quite so critical, provided that the surface sulfur reaches the oxidation state +6 (4, 7);

(ii) it is strictly necessary that the sulfation process is carried out on amorphous Zr hydroxide, and not on crystalline ZrO_2 phase (4, 8–11).

It has been also reported that the crystallization of ZrO_2 subsequent to the sulfation process and delayed by the presence of sulfates, is probably necessary for the development of an appreciable catalytic activity. The crystallization process ought to occur in the presence of an adequate (i.e., high) amount of sulfates, whereas sulfated samples, obtained by direct sulfation of any crystalline ZrO_2 phase, would remain catalytically inactive (4, 11).

Previous work from the authors of this article was devoted to the identification of some of the surface chemical and catalytic features of different s.d.-ZrO_2 systems (6, 12, 13), but the amorphous/crystalline state of ZrO_2 has not yet been considered in detail. In order to contribute to a better understanding of the catalytic properties of s.d.-ZrO_2 systems, the present work deals with the relationship between the crystal phase of the ZrO_2 support and the spectroscopic features and/or catalytic activity exhibited by the resulting s.d.-ZrO_2 system.

EXPERIMENTAL

Materials

Several families of s.d.-ZrO_2 systems have been considered, and their preparative features can be summarized as follows.

0021-9517/95 $12.00

Monoclinic samples. A mostly monoclinic ZrO_2 system, designated in the text and figures by ZRP, was obtained by the hydrolysis with pure water of Zr-propoxide (15). The resulting amorphous hydroxide was calcined in air at a temperature that is designated by a subscript numeral ($T_1 \geq 673$ K). Surface sulfation of the precalcined ZRP_{T_1} powders was carried out either with H_2SO_4 (≈ 0.5 *N*) or with $(NH_4)_2SO_4$, followed by calcination in air at a temperature $T_2 \geq 673$ K, in order to eliminate the unreacted acid or to decompose the ammonium sulfate. The sulfation procedure is indicated in the samples symbol by the letter H (from sulfuric acid) or N (from ammonium sulfate), respectively, and the letter is preceded by another numeral, *n*, which represents the sulfates concentration achieved (S atoms per nm^2). (E.g., the symbol $ZRP_{873}[3.3N]T_2$ stands for a sample of (mostly) monoclinic ZrO_2, precalcined at 873 K, sulfated with ammonium sulfate and containing, after the calcination at a certain temperature T_2, 3.3 sulfate groups per nm^2. The plain symbol ZRP_{T_1} stands for the precursor material, i.e., the nonsulfated starting material calcined in air at T_1.)

ZS samples. These are standard s.d.-ZrO_2 catalysts, that we have used previously and described in previous notes (12–14, 16). The catalysts have been prepared following the procedure indicated by the Japanese school as the only procedure leading to superacidity (4, 8), i.e., by sulfating (usually with ammonium sulfate) an amorphous Zr hydroxide precursor. In our case, the precursor Zr hydroxide was obtained by the sol-gel technique, as described in a previous note (13). ZS samples are designated in the text by their symbol, followed by a bracket reporting the surface concentration of sulfates (*n*; S atoms per nm^2) and by the letter H or N, which designates the sulfation procedure adopted. The bracket is then followed by a numeral T_2, corresponding to the temperature (K) at which the sulfated amorphous precursor was calcined in air. (E.g., the symbol ZS[2.6N]823 stands for a catalyst that was prepared by the impregnation with ammonium sulfate of a sol-gel Zr hydroxide precursor, and that contains, after calcination at 823 K, 2.6 sulfate groups per nm^2. Neither a symbol nor any data are reported for the precursor of the ZS samples, as it corresponds to a completely amorphous Zr hydroxide, as shown for instance in Ref. [7].)

Tetragonal samples. The tetragonal modification of ZrO_2 is known to be metastable at low temperatures, and to coexist with the stable monoclinic modification only if the crystallites are small ($d \leq \approx 30$ nm) (17), whereas it becomes the stable ZrO_2 phase at temperatures higher than ≈ 1500 K. Ninety-eight percent pure tetragonal ZrO_2 specimens, stable at all temperatures up to ≈ 1300 K, have been obtained by the phase stabilization brought about by the formation of a solid solution with ≈ 3 mol% Y_2O_3, following a preparative procedure described elsewhere (18). For our Y-stabilized tetragonal ZrO_2 samples, termed TO3, XPS data indicate that, after firing at temperatures as high as ≈ 1173 K, Y_2O_3 is regularly dispersed within the solid solution and does not accumulate nor segregate at the surface.

For the present study, TO3 specimens have been precalcined in air and crystallized in the tetragonal form at $973 \geq T_1 \geq 693$ K, and have been then sulfated with either sulfuric acid or ammonium sulfate. The catalysts were eventually calcined in air at $T_2 \geq 673$ K. Sulfated tetragonal ZrO_2 samples are designated in the text by their symbol (TO3), followed by the subscript T_1, by a bracket reporting the surface concentration of sulfates (*n*; S atoms per nm^2) and containing the letter H or N that refers to the sulfation procedure, and eventually by the T_2 referring to the calcination step. (E.g., the symbol $TO3_{873}[2.9N]923$ stands for a specimen of Y_2O_3-stabilized tetragonal ZrO_2, crystallized in air at 873 K, sulfated with ammonium sulfate and containing, after the calcination in air at 923 K, 2.9 sulfate groups per nm^2. The plain symbol $TO3_{T_1}$ stands for the precursor material, i.e., the nonsulfated starting material, calcined in air at T_1.)

Techniques

The sulfate concentrations of all s.d.-ZrO_2 were determined by alkaline extraction and ionic chromatography, as described elsewhere (16).

Catalytic activity was studied in a quartz flow reactor (i.d. = 8 mm) heated by an external oven. The system was operated at the following conditions: reaction temperature 423 K; total pressure 1 atm; *n*-butane : helium = 3 : 1; total space velocity = 200 h^{-1}. Prior to reaction, the catalyst (1.5 g; 100–120 mesh) was activated *in situ* at 723 K in a dry air flow for 2 h, and then cooled to the reaction temperature (423 K). All reactant and product gas concentrations were measured on line by gas chromatography. Reaction rates were defined as moles of *n*-butane converted per mole SO_4 in the sample per unit time.

IR spectra were run at resolution 2 cm^{-1} with a Bruker 113v FTIR spectrometer equipped with MCT detector. S.d.-ZrO_2 samples were prepared for IR measurements in the form of thin-layer depositions (≈ 5 mg per cm^2), spread from aqueous suspensions over a pure Si platelet. The samples were then transferred to a quartz vacuum cell, where they underwent a first vacuum activation/oxidation process at 673 K and all other subsequent thermal and/or adsorption treatments described in the text in a strictly *in situ* configuration.

BET surface area measurements were carried out with N_2 at 77 K on a Carlo Erba 1900 Sorptomatic apparatus.

XRD patterns were obtained for all pure and s.d.-ZrO_2 specimens with a Philips PW 1820 diffractometer, using Cu$K\alpha$ radiation.

TABLE 1

Structural and Morphological Features of Some ZrO_2 and s.d.-ZrO_2 Specimens

	Sample	$BET_{s.a.}$ (m^2g^{-1})	Texture	Crystal phase
A	ZRP_{873}	55	Crystallites of ≈ 20–40 nm	m (40–70%)
B	ZRP_{873} [3.3 N] 823	55	Crystallites of ≈ 20–40 nm	m (93%)
C	ZRP_{873} [2.8 N] 923	48	Crystallites of ≈ 20–40 nm	m (94%)
D	ZRP_{873} [3.55 H] 673	55	Crystallites of ≈ 20–40 nm	m (78%)
E	ZRP_{873} [3.5 H] 773	55	Crystallites of ≈ 20–40 nm	m (78%)
F	ZRP_{873} [2.75 H] 923	50	Crystallites of ≈ 20–40 nm	m (80%)
G	ZRP_{1073}	24	Crystallites of ≈ 35–60 nm	m (92%)
H	ZRP_{1073} [1.3 H] 773	24	Crystallites of ≈ 35–60 nm	m (92%)
I	ZS [1.85 N] 673	230	Polyaggregate nanocrystals	(quasi-) t
J	ZS [2.6 N] 823	188	Crystallites of ≈ 5–10 nm	t
K	ZS [1.5 N] 923	128	Crystallites of ≈ 10–12 nm	t
L	$TO3_{873}$	85	Crystallites of ≈ 10–15 nm	t
M	$TO3_{873}$ [5.75 N] 673	85	Crystallites of ≈ 10–15 nm	t
N	$TO3_{873}$ [4.65 N] 823	85	Crystallites of ≈ 10–15 nm	t
O	$TO3_{873}$ [2.7 N] 923	80	Crystallites of ≈ 10–15 nm	t

Note. m, monoclinic ZrO_2; t, tetragonal ZrO_2.

High-resolution transmission electron micrographs were obtained with a Jeol JEM 2000 EX microscope, equipped with a top-entry stage; all samples were dispersed in *n*-heptane and then deposited from the suspension on holey carbon Cu grids.

RESULTS AND DISCUSSION

In order to assess the importance of the ZrO_2 crystal phase to the surface features and to the catalytic activity of s.d.-ZrO_2, it has been necessary to examine a very large number of systems, and each system has been examined under various conditions (i.e., varying several parameters, like T_1, T_2, and n).

Table 1 summarizes symbols, structural data and texture features of just a few significant s.d.-ZrO_2 samples, out of the many examined. These are the samples that will be considered in the forthcoming discussion.

For the sake of clarity, the correlations between the ZrO_2 crystal phase and various surface properties of s.d.-ZrO_2 catalysts will be considered separately.

A. Does the Sulfation Process Affect the ZrO_2 Crystal Phase?

Figures 1 and 2 report high-resolution TEM images and XRD patterns, respectively, of some of the s.d.-ZrO_2 preparations, the features of which are presented in Table 1.

ZRP samples. Figure 1a shows that the starting preparation ZRP_{873} (sample A) is a well-crystallized system, made up of well-separated roundish thin particles of 20–40 nm diameter. The particles are mainly isooriented, and present top terminations with extended regular patches of few low-index crystal planes that can be identified with reasonable accuracy from the fairly regular patterns of interference fringes. The corresponding XRD trace 2a confirms the good crystallinity of the sample, and indicates that a large proportion of the sample is still made up of crystallites belonging to the tetragonal phase. The proportion of tetragonal-to-monoclinic phase was determined by the formula proposed by Evans *et al.* (19); for instance, for ZRP treated at T_1 = 873 K, the proportion was observed to vary between some 60 and 30%, depending on the firing rate and time.

The coupled pictures presented in Figs. 1b and 1c are relative to two ZRP_{873} T_2 samples sulfated via ammonium sulfate (specimens B and C, respectively), whereas the pictures in Fig. 1d and 1e are relative to two corresponding ZRP_{873} T_2 samples sulfated via sulfuric acid (specimens D and F, respectively). It can be noted that both sulfation processes have little effect (if any) on the texture, size, and morphology of ZrO_2 crystallites. The side terminations of the crystallites have possibly become more roundish (i.e., more defective) as a consequence of the attack by the sulfating agents, but the crystallites are still well separated and maintain the original form of very thin platelets. This is demonstrated by the frequent appearance in the micrographs of Moirè fringes. The particles size distribution is left virtually unchanged by either sulfation process, and also by a calcination at T_2 = 923 K (i.e., at a temperature slightly higher than the temperature T_1 of the first thermal treatment); this is consistent with a very limited decrease

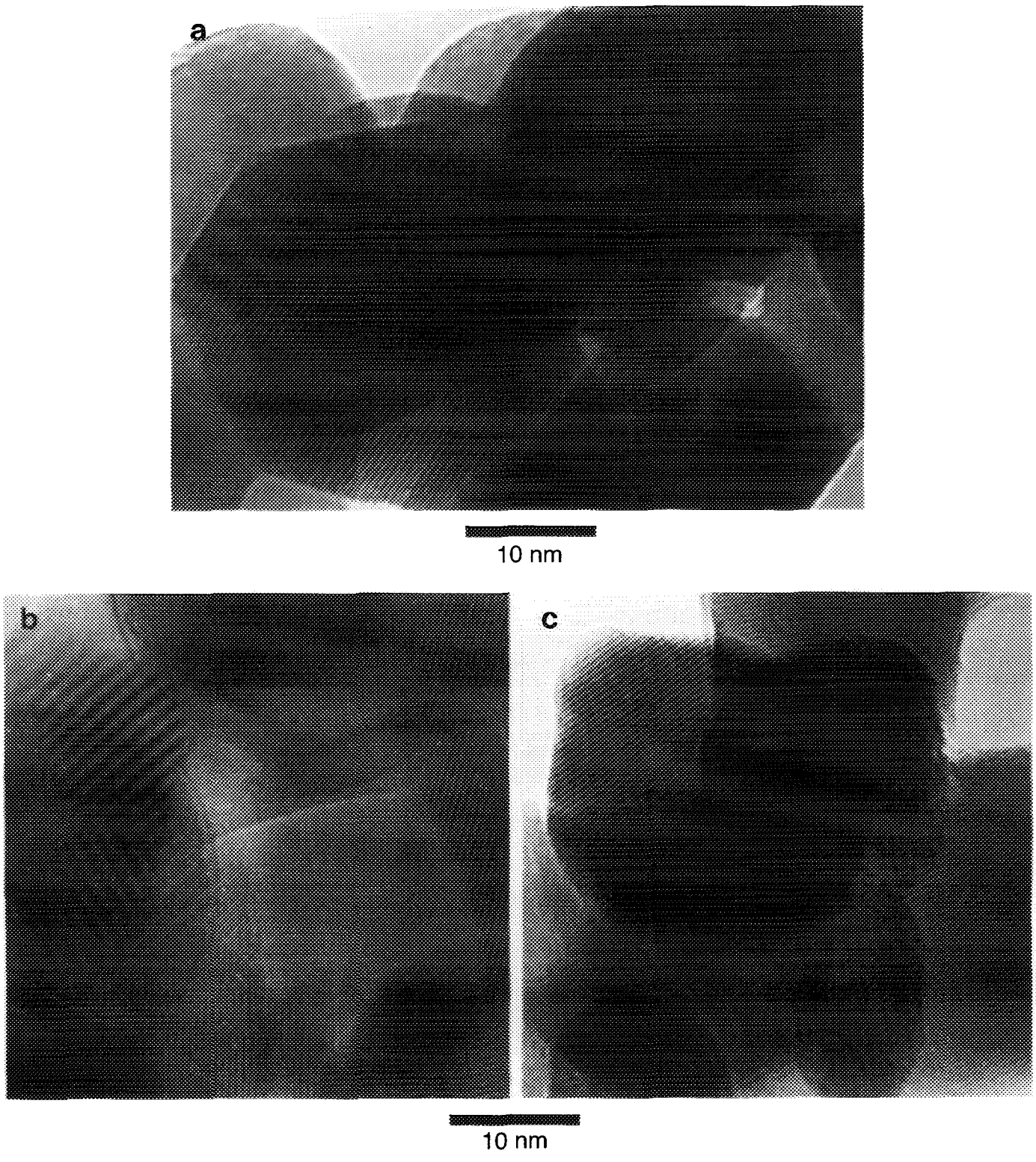

FIG. 1. High-resolution transmission electron micrographs of some ZrO_2 and s.d.-ZrO_2 specimens. (a) ZRP_{873} (sample A); (b) ZRP_{873}[3.3N]823 (sample B); (c) ZRP_{873}[2.8N]923 (sample C); (d) ZRP_{873}[3.55H]673 (sample D); (e) ZRP_{873}[2.75H]923 (sample F); (f) ZRP_{1073} (sample G); (g) ZS[1.85N]673 (sample I); (h) ZS[2.6N]823 (sample J); (i) ZS[1.5N]923 (sample K); (j) $TO3_{873}$ (sample L); (k) $TO3_{873}$[2.7N]923 (sample O).

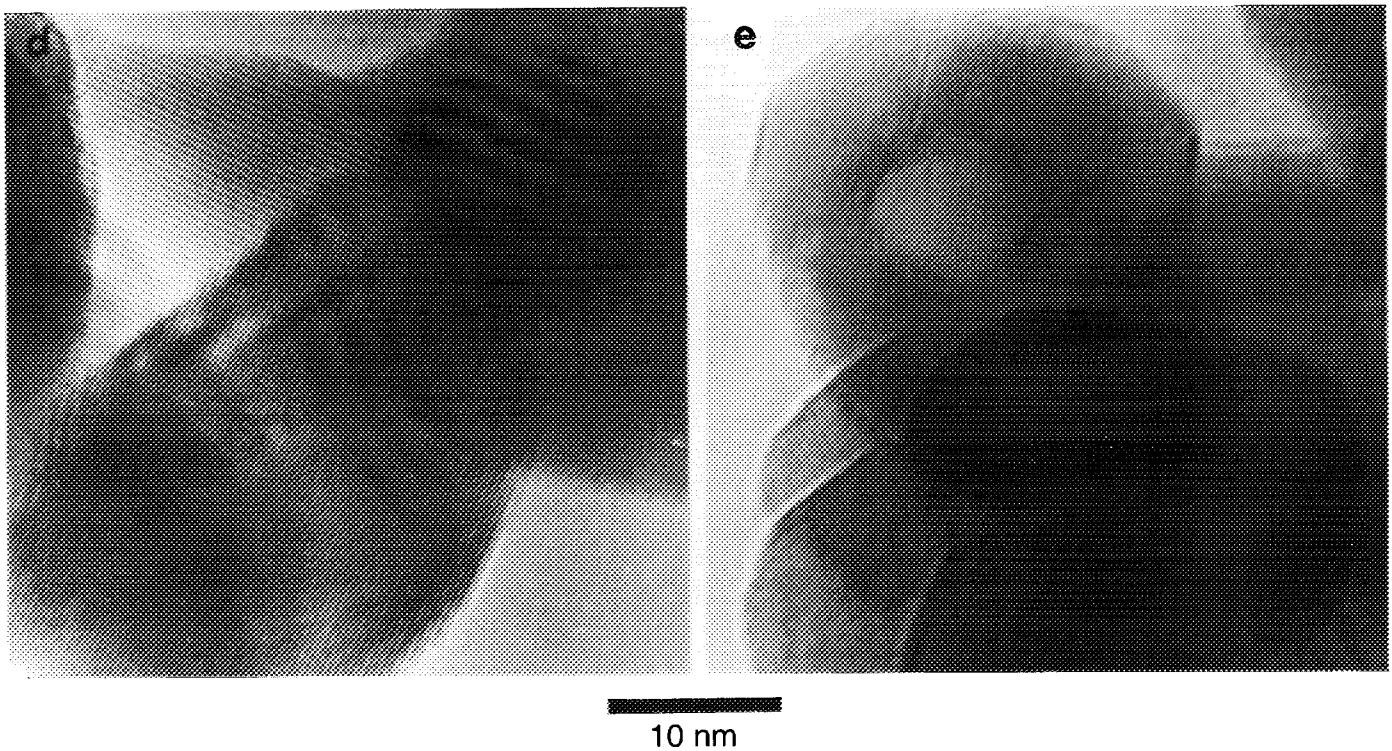

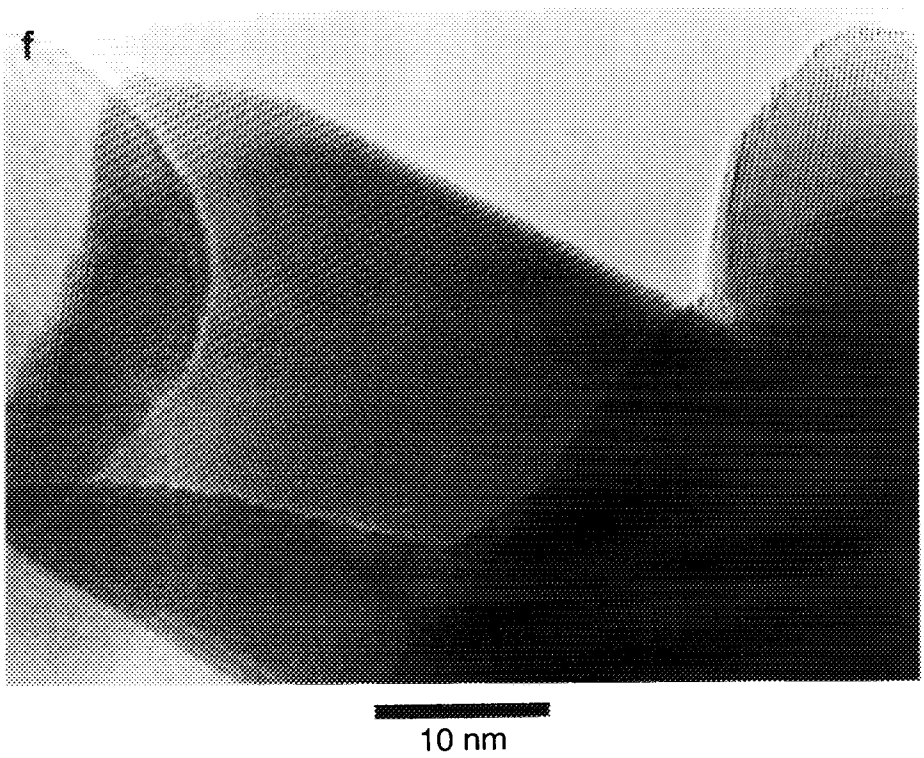

FIG. 1—*Continued*

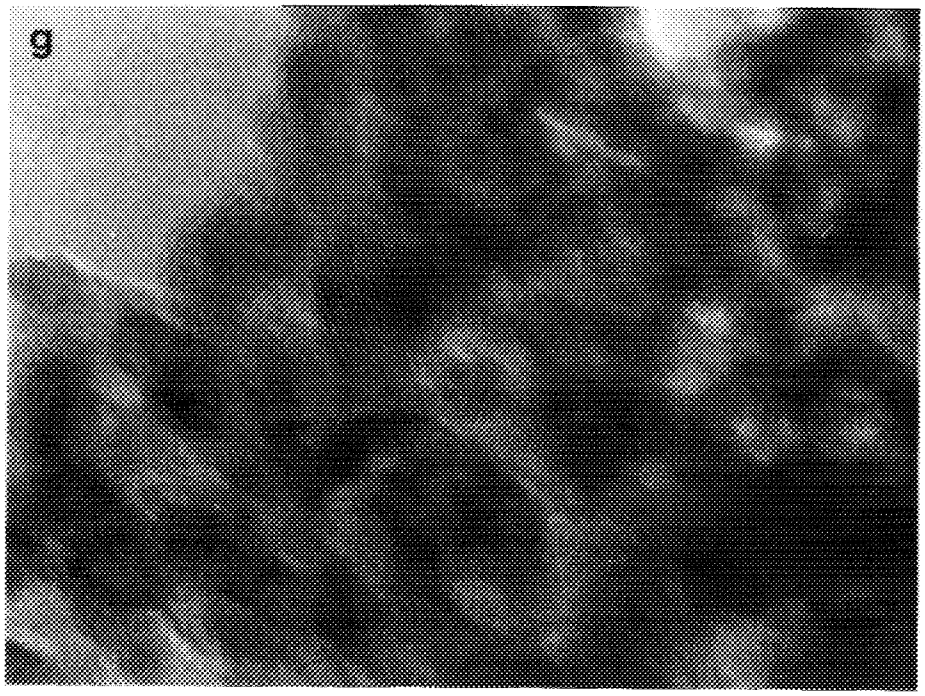

FIG. 1—*Continued*

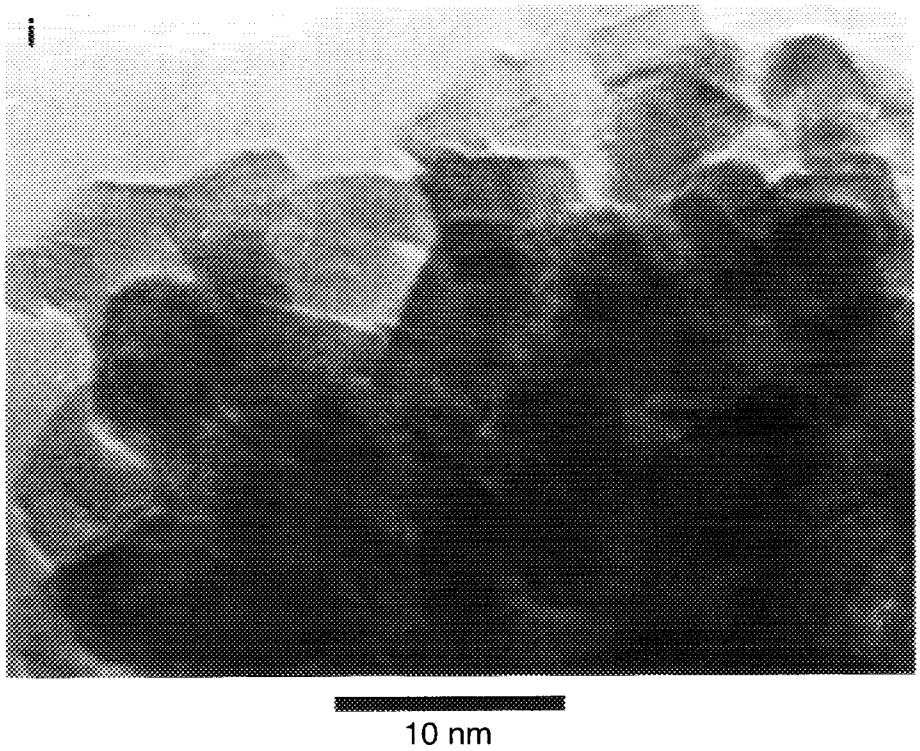

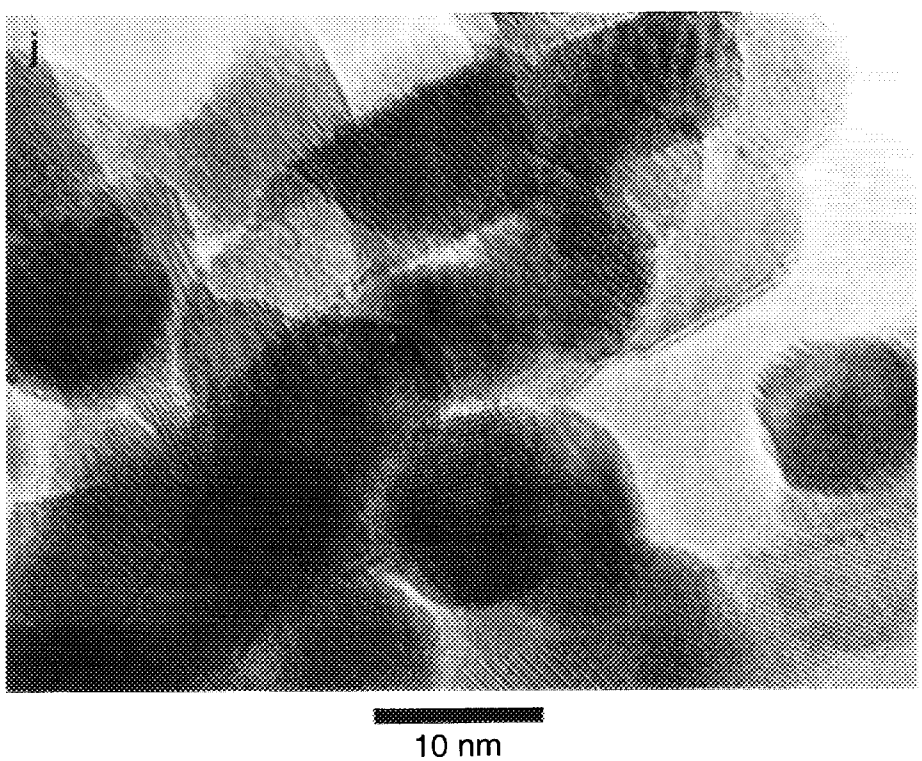

FIG. 1—*Continued*

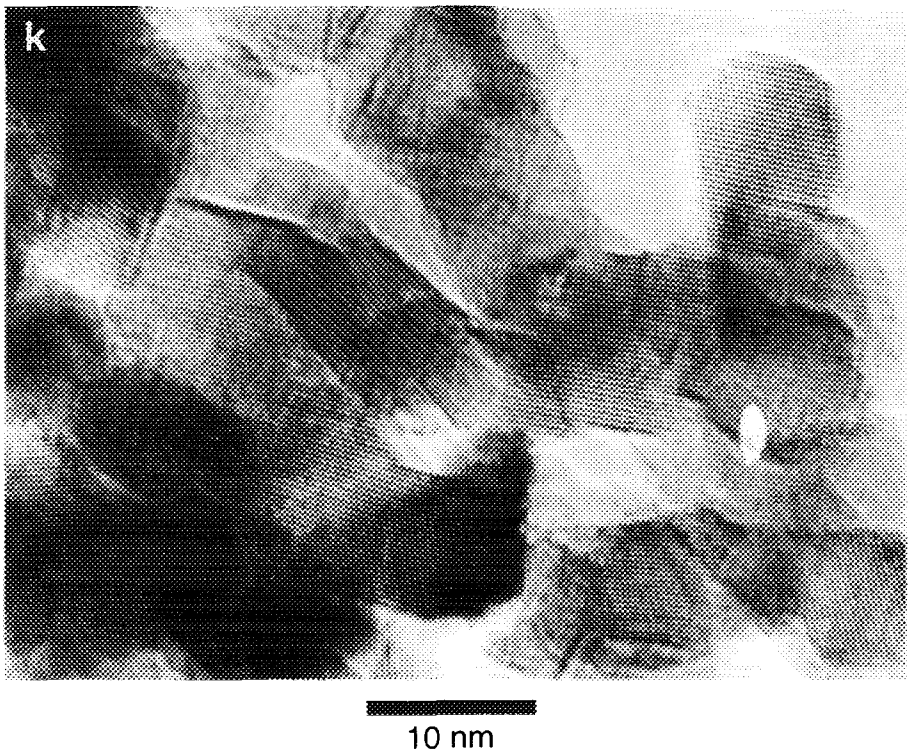

FIG. 1—*Continued*

of BET surface area exhibited by these s.d.-ZrO_2 systems, and reported in Table 1.

The XRD patterns of Fig. 2b (relative to sample B) and Fig. 2c (relative to sample D) indicate that, unlike the particle shape and size distribution, the crystal-phase distribution of crystalline ZRP_{873} specimens is affected strongly by the sulfation processes, as the percentage of the tetragonal ZrO_2 form decreases dramatically upon sulfation. In particular, the sulfation via ammonium sulfate virtually eliminates the tetragonal ZrO_2 component, whereas no more than 10–15% of the tetragonal form remains after sulfation via sulfuric acid. The thermal treatment at temperatures T_2 as high as 923 K (i.e., at $T_2 \geq T_1$) has no further appreciable effect on the crystal-phase distribution.

The result concerning the ZrO_2 phase distribution upon sulfation is quite unexpected (though consistent with the behaviour reported previously for a quasi-crystalline (monoclinic) ZrO_2 preparation (6)). In fact, several authors have demonstrated that the sulfation process, when carried out on the amorphous hydrated ZrO_2 phases, tends to favour the metastable tetragonal form, and this observation will indeed be confirmed in the next section. Unlike that, here it is observed that sulfation of a mixed-phase crystalline ZrO_2 preparation favours the conversion of the metastable form into the thermodynamically stable monoclinic form, also in the absence of an appreciable growth of the average size of crystallites (17).

Figures 1f and 2d present, for comparison, the morphology and the XRD pattern of a ZRP_{1073} specimen (sample G), in which a higher firing temperature T_1 brought about:

(i) appreciable growth of the average crystal size ($d \approx$ 35–60 nm);

(ii) the creation of more regular side terminations of the crystallites. In fact, the particles still terminate with flat and extended patches of low-index crystal planes, but the edges are now more regular and far sharper;

(iii) the virtually complete transformation of the metastable tetragonal form into the monoclinic one. After treatment with either sulfuric acid (sample H, not shown in the figure) or ammonium sulfate, it was observed that the sulfation process does not modify the morphology of the well-crystallized system, and does not modify any further the ZrO_2 crystal-phase distribution that has already reached a stable ratio.

ZS samples. Sections g–i of Fig. 1 show the high-resolution images of three ZS samples (specimens I, J, and K, respectively) treated at increasing T_2 temperatures. Sections e–g of Fig. 2 show the corresponding XRD patterns. The present morphological and crystallographic data confirm what was previously suggested by several authors; sulfation of amorphous Zr hydroxide precursors stabilizes particles of small size (i.e., high BET surface areas) and, when crystallization occurs, the small particles size stabilizes the (sole) tetragonal ZrO_2 phase.

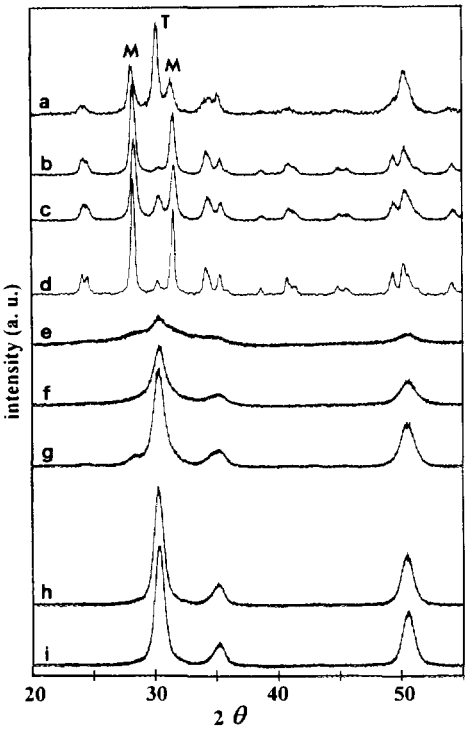

FIG. 2. Segments of the X-ray diffraction patterns of some ZrO_2 and s.d.-ZrO_2 specimens. (a) ZRP_{873} (sample A); (b) ZRP_{873}[3.3N]823 (sample B); (c) ZRP_{873}[3.55H]673 (sample D); (d) ZRP_{1073} (sample G); (e) ZS[1.85N]673 (sample I); (f) ZS[2.6N]823 (sample J); (g) ZS[1.5N]923 (sample K); (h) $TO3_{873}$ (sample L); (i) $TO3_{873}$ [2.7N]923 (sample O). The letters "M" and "T" stand for monoclinic and tetragonal reflexes, respectively.

A relatively new aspect is evidenced by Fig. 1g (sample I); with this preparation, the presence of sulfates does not delay appreciably the amorphous-to-crystalline transition, in contrast with what observed before (4). In fact, the sample treated at T_2 = 673 K (sample I) also turns out to be already microcrystalline. The TEM images show the presence in sample I of an ill-defined network of polyaggregate particles with a quasi-circular cross section (≈5 nm diameter), in which small and disorderly distributed patterns of interference fringes are observable. This indicates that small domains of regularly spaced crystal planes are already being formed. It is possible that the specimens of ZS[1.85N]673 (sample I), when observed with the electron microscope, became more crystalline due to the heating effect caused by the high-energy electron beam. But the XRD trace of Fig. 2e also shows that this preparation should no longer be considered plainly amorphous, but rather as a nanocrystalline tetragonal ZrO_2 phase.

Firing the ZS specimens at temperatures as high as 923 K (Fig. 1h and 1i) brings about the fast separation of individual particles, and their gradual growth. The tiny particles maintain to various extents a quasi-circular shape (this is far more evident in sample J than in sample K), that is indicative of a high incidence of some crystallographically defective configurations constituting the round crystal edges. At the same time, the top termination of the particles presents interference fringes that are progressively more clearly defined, indicative of the gradual development of a regular flat termination of the crystallites along regular crystal planes. In agreement with the separation and growth of individual particles, the surface area declines quickly (see Table 1), though still remaining much higher than the surface area of any of the systems that were allowed to crystallize before sulfation.

TO3 samples. The electron micrograph of the reference nonsulfates Y-stabilized tetragonal ZrO_2 system (sample L) is shown in Fig. 1j, and the corresponding XRD pattern is reported as trace h in Fig. 2. The material is well crystallized, with well-separated individual crystallites. The scale-like morphology of TO3 is quite similar to that of the ZRP (monoclinic) preparation, but:

(i) the average size of the crystallites is smaller ($d \approx$ 10–15 nm);

(ii) the contours are somewhat less roundish (i.e., there should be a relatively lower incidence of crystallographically defective configurations);

(iii) the crystalline form is purely tetragonal.

Sulfation of the TO3 preparation (by either sulfation procedure) followed by thermal treatment at T_2 as high as 923 K (see, for instance, sample O, in Figs. 1k and 2i) does not modify to an appreciable extent the average crystal size nor the particle shape (only the side terminations became possibly sharper with sulfation and calcination at 923 K). The crystalline form of the ZrO_2 support remains purely tetragonal, as it does when the thermal treatment of the sulfated system occurs at a temperature slightly higher than temperature T_1 of the preparation step. This indiciates that the phase stabilization of the tetragonal ZrO_2 form, brought about by 3 mol% Y_2O_3 dispersed in the solid solution, is more efficient than all possible phase destabilizing effects. The latter may be produced by:

(i) calcination at a temperature T_2 as high as 923 K (in fact, it is known that high firing temperatures favour the monoclinic phase of ZrO_2);

(ii) the creation of more than a statistical monolayer of sulfate groups at the surface of the TO3 material (In fact, sulfation was shown above to eliminate the tetragonal ZrO_2 component in the mixed ZRP preparations).

It is here recalled that an average monolayer of SO_4 groups corresponds to ≈4 groups per nm^2 (5).

B. Do the Features of Surface Sulfates Depend on the ZrO_2 Crystal Phase?

It has been shown in several works (e.g., see (13, 20)) that surface sulfates on s.d.-ZrO_2, as well as on other sul-

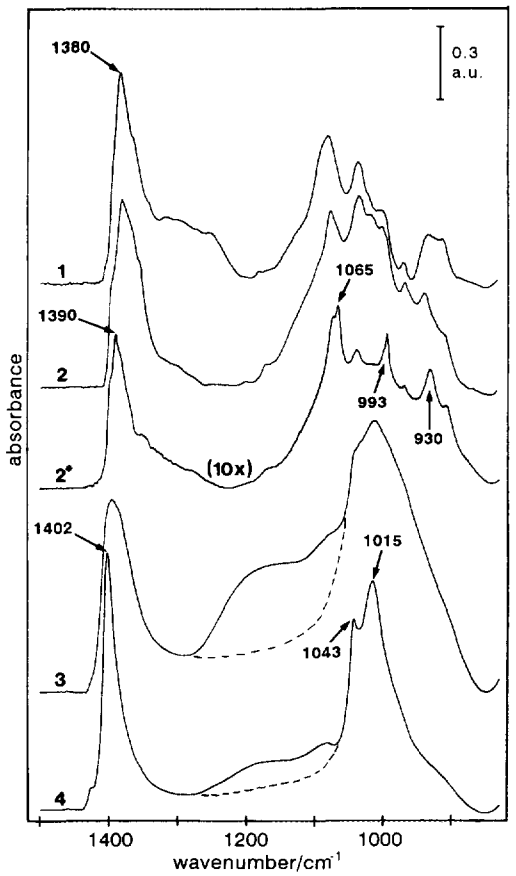

FIG. 3. Absorbance IR spectra in the ν(SO) vibrations region of some s.d.-ZrO_2 specimens. (1) ZRP_{873}[2.8N]923 (sample C); (2) ZRP_{873}[2.75H]923 (sample F); (2*) (inserted for comparison): ZRP_{1073}[1.3H]773 (sample H); (3) ZS[2.6N]823 (sample J); (4) $TO3_{873}$[2.7N]923 (sample O). (The spectrum of curve 2* underwent a 10-fold ordinate scale magnification).

fated oxidic systems, can assume different structures with varying surface hydration degree. In particular, on materials brought to medium-high dehydration stages (this condition is necessary for catalytic activity), surface sulfates tend to acquire a highly covalent structure and spectral features somewhat similar to those characteristic of sulfones or organic sulfates (21). In the present paper, the ultimate comparison among different s.d.-ZrO_2 preparations will be carried out on the catalytic ground of the isomerization reaction of *n*-butane; since the best catalytic behaviour is exhibited by active s.d.-ZrO_2 systems after vacuum (or dry air) activation at $T \geq 623$ K, we will consider only the spectral features of surface sulfates present on the various s.d.-ZrO_2 preparations after *in situ* vacuum activation at 673 K.

Curves 1–4 of Fig. 3 report the spectral region of the ν(SO) vibrations of surface sulfates on four different s.d.-ZrO_2 systems, characterized by very similar sulfate concentrations ($\approx$2.7 S atoms per nm^2). Curves 1 and 2 refer to two ZRP_{873} specimens sulfated by the two sulfation methods (samples C and F, respectively), curve 3 is relative to a typical ZS preparation (sample J), and curve 4 represents a $TO3_{873}$ system (sample O). The overall spectral features of the four samples are quite similar: all samples exhibit strong bands in the range 1430–1300 cm^{-1} (due to $\nu_{S=O}$ vibrations) and in the range 1150–850 cm^{-1} (due to ν_{S-O} vibrations). Still, the detailed spectral structure of sulfates presents appreciable differences.

(i) The spectra of the two monoclinic ZRP_{873} samples (curves 1 and 2) are very similar and so confirm the negligible role played (at least in this respect) by the sulfation procedure. They present a complex $\nu_{S=O}$ band partly resolved into several components, none of which is at $\nu \geq 1400$ cm^{-1}, whereas the $\nu_{S=O}$ absorption is split into several resolved components ranging between $\approx$1100 cm^{-1} and $\approx$900 cm^{-1}. In particular, some of the latter bands are well resolved and absorb quite strongly at $\nu \approx 1080$ cm^{-1} and at $\nu \leq 970$ cm^{-1}. Bensitel *et al.* (19) analyzed in detail the various bands characteristic of sulfates at the surface of a (mainly) monoclinic ZrO_2 system similar to the present one, and concluded that (at least) three slightly different sulfate species of similar structure were present, possibly located in different crystallographic situations. The $\nu_{S=O}$ spectral components resolved at $\approx$1080 and at 900–950 cm^{-1} are most likely correlated, and turn out to be characteristic of (some of) the covalent sulfate species formed at the surface of monoclinic ZrO_2. The spectrum inserted for comparison as trace 2* in Fig. 3 is relative to the sample ZrP_{1073}[1.3H]773 (specimen H); it indicates that, on this sintered preparation, the $\nu_{S=O}$ sulfate modes at $\approx$1070 and $\approx$930 cm^{-1} are by far predominant, and are also correlated with a third sharp component at $\approx$990 cm^{-1}. These three $\nu_{S=O}$ components are thus ascribed to covalent sulfates formed on regular low-index crystal planes of the monoclinic ZrO_2 phase. In fact, this type of termination is by far predominant in the case of ZRP systems presintered at relatively high temperatures (see Fig. 1f), and the crystal face most favourably exposed is the (111) plane (22).

(ii) The spectra of sulfates of the tetragonal ZrO_2 preparations (curves 3 and 4) are fairly similar, in spite of the very different preparative procedures. The spectra are also quite different from those of the monoclinic ZrO_2 phase. This indicates that the crystallographic form of ZrO_2 is of primary importance in determining the structure and geometry of surface anionic species. It is here recalled that the same conclusion could be drawn considering the carbonate-like species formed at the surface of monoclinic and tetragonal ZrO_2 upon CO_2 uptake (23, 24).

In both tetragonal preparations the spectrum of sulfates is dominated by two main features; there is a strong and unresolved $\nu_{S=O}$ component centered at $\nu \approx 1400$ cm^{-1} (the

band presents a largely variable asymmetric broadening on the low-wavenumber side), and there is a strong $\nu_{S=O}$ absorption at 1050–1000 cm^{-1} that is clearly resolved, though to a different extent, into two components. These features can be possibly ascribed to two slightly different families of covalent sulfates of the same type. They would be formed, for instance, on regular crystal planes of *t*-ZrO_2 (the bands at ≈1400 and ≈1020 cm^{-1}) and on crystallographic defects (the broad tailing at ≈1380 cm^{-1} and the band at ≈1040 cm^{-1}).

These sulfate species, that present only a couple of strong bands in the 1450–850 cm^{-1} range, are by far the prevailing sulfate species formed on tetragonal ZrO_2 systems. They correspond to sulfate species present to a much lower extent (if at all) at the surface of the monoclinic ZrO_2 preparations. On the other hand, the sulfate species prevailing on monoclinic systems, and characterized by $\nu_{S=O}$ modes at $\nu < 1380$ cm^{-1} and by several resolved $\nu_{S=O}$ modes between ≈1080 and 900 cm^{-1}, are virtually absent on tetragonal ZrO_2 specimens.

The different spectral features of covalent sulfates formed on the dehydrated surface of the two ZrO_2 phases indicate different geometries and, possibly, a different covalent character of the two families of surface anions. It is recalled that the two crystalline modifications of ZrO_2 have different lattice parameters, different coordination number of the Zr^{4+} ions, and tend to expose different crystal planes (18).

The main feature that sulfates at the surface of the two ZrO_2 phases have in common is the presence of a single S=O stretching vibration, separated by 300–400 cm^{-1} from the S–O stretching vibration(s). This fact was interpreted by Bensitel *et al.* (20) as due to the presence of $(O)_3-S=O$ surface structures, rather than

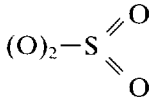

structures, and their assignment agrees with isotopic substitution data obtained by the same authors. However, their assignment conflicts with the oxidation state +6 observed by several authors for surface sulfur on catalytically active s.d.-ZrO_2 systems, and with the observation that the S=O stretching mode of organic sulfites is appreciably lower in frequency than the stretching of organic sulfates (25). On the other hand, no coupled O=S=O vibrations can be responsible for the two strong bands at ≈1400 and ≈1000 cm^{-1}. In fact, the spectral splitting observed is much too large; the symmetric ν_{SO_2} vibration, coupled with an asymmetric vibration at ≈1400 cm^{-1}, should be expected in the 1250–1150 cm^{-1} range (21, 25). In the latter range, additional bands of variable intensity are indeed observed on some samples, and in some conditions (e.g., see the spectral segments evidenced by the broken lines in curves 3 and 4 of Fig. 3). The presence of O=S=O surface groups was postulated by other authors and is more compatible with the oxidation state +6 of surface S; if O=S=O groups are responsible for the sole $\nu_{S=O}$ vibration at ≈1400 cm^{-1}, they must possess a bond angle very close to 90°. This should apply at least to the tetragonal ZrO_2 phase, on which the dominant sulfate species presents only two strong bands, one with clear $\nu_{S=O}$ character and the other with ν_{S-O} character. As for the monoclinic ZrO_2 phase, the main difference consists in a higher number and a different spectral location of the ν_{S-O} modes (as imposed by a different geometry and a different coordination number of cations); for this phase, the $(O)_3-S=O$ structure proposed by Bensitel *et al.* (20) may possibly be correct.

C. Does the Catalytic Activity Depend on the ZrO_2 Crystal Phase?

Figure 4 reports, in separate sections, the *n*-butane isomerization activities on various specimens of the three families of s.d.-ZrO_2 systems. It is quite evident that the overall shape of the activity plots varies from sample to sample, especially in the first part of the plots (corresponding to the first ≈30 min of reaction), and this depends on the nature and extent of concurrent side reactions. This aspect is not pertinent here, and will be discussed elsewhere.

In the present work and for the present purpose, we may concentrate our attention on the sole plateau section of the activity plots. For instance, the rate of *n*-butane conversion into isobutane at $t = 100$ min gives a valid tool of comparison for the specific catalytic activity of the various materials. The "normalization" of the conversion observed with the various catalysts has been done per mole SO_4 in the sample per unit time. This procedure yields an "absolute" value for the catalytic activity only within the limits of the underlying assumption that *all* sulfate groups are equivalent and participate in the reaction. Actually, data reported in this work (see below) as well as in previous works (16) indicate that the amount of sulfur is *not* an absolute measure of the amount of active sulfur. On the other hand, normalization of conversion against BET surface area would also yield a questionable "absolute activity," as the systems are quite heterogeneous, and the phenomena on regular crystal faces and on crystallographically defective configurations are not equivalent.

ZRP samples. Monoclinic ZrO_2 specimens (Fig. 4a), sulfated by any sulfation method, turn out to possess either very small or null catalytic activity. This is consistent with the general statement reported by several authors that sulfating crystallized ZrO_2 yields virtually inactive catalysts.

No matter what the starting sulfate surface loading, mild

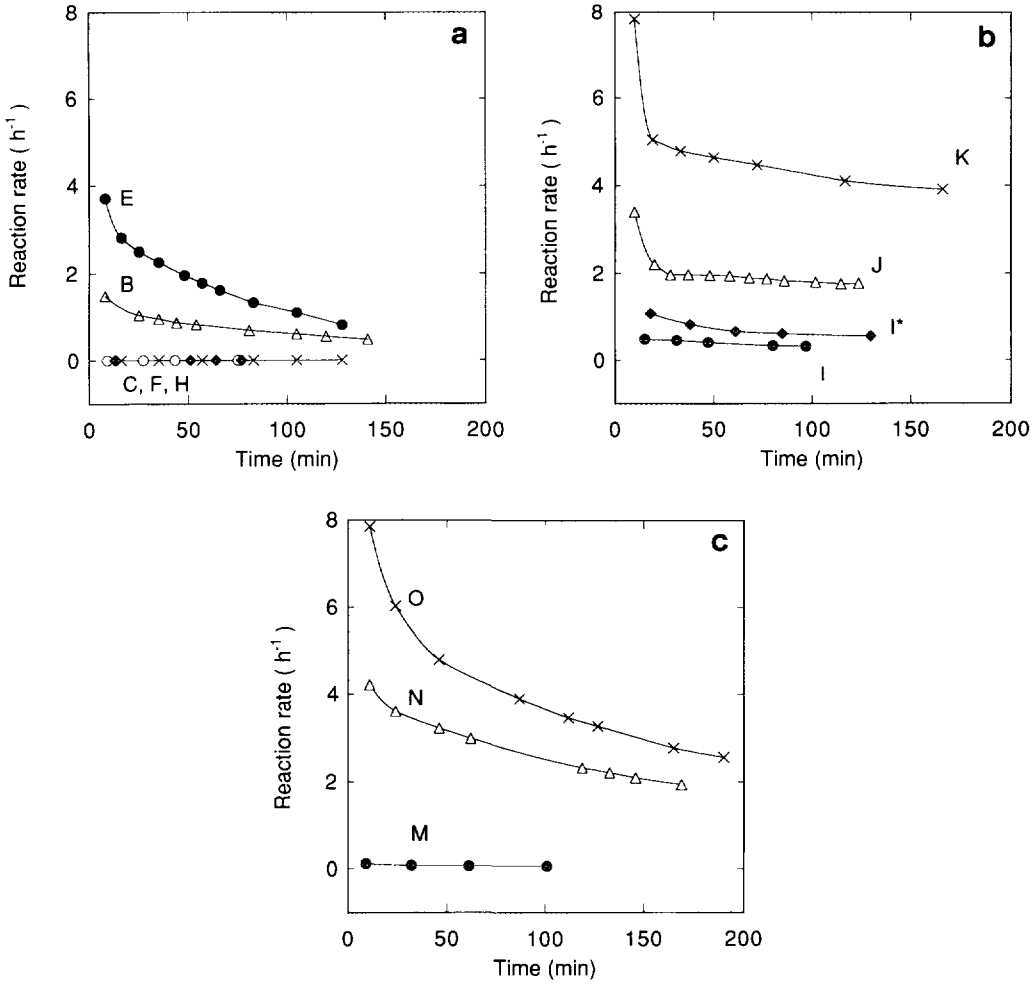

FIG. 4. *n*-Butane isomerization activity at 423 K as a function of time on stream for s.d.-ZrO_2 systems activated at 673 K. (a) ZRP catalysts. (b) ZS catalysts. (c) TO3 catalysts. The capital letters on the curves designate the several s.d.-ZrO_2 samples, as shown in Table 1. The curve marked I* in b is relative to the sample ZS[2.85N]773, not reported in Table 1, intermediate between the ZS samples I and J.

activations of ZRP_{873} samples at T_2 as high as 773–823 K still allow a small catalytic activity of no practical interest (see the traces of samples B and E in Fig. 4a), whereas activations at T_2 (even slightly) higher than 823 K lead to inactive systems (see traces C and F).

The spectra of sulfates reported in Fig. 5 show that, in the activation temperature interval T_2 = 673–923 K, mainly a fraction of sulfates absorbing at ≈1400 and ≈1395 cm^{-1} ($\nu_{S=O}$ modes) and at ≈1065–1090, ≈990, and ≈930 cm^{-1} (ν_{S-O} modes) are eliminated (see, in particular, the differential spectrum (3-1) of Fig. 5). It is thus suggested that this small fraction of sulfates, belonging to the large family of sulfates tentatively ascribed to regular crystal planes, is responsible for the minor catalytic activity exhibited by some of the monoclinic s.d.-ZrO_2 systems. However, it is confirmed that a necessary condition for the development of a catalytic activity is the presence of surface sulfates of the highest covalency, characterized by a $\nu_{S=O}$ mode at $\nu \geq 1390$ cm^{-1}.

The catalytic activity of monoclinic ZrO_2 specimens crystallized before sulfation at high T_1 temperatures (e.g., see the case of sample H, shown in Fig. 4a) is in general null, unless very high sulfate loadings ($n > 4$ groups per nm^2) are used. But in the latter case, the thermal stability of the surface sulfates layer is very low, and the catalyst deactivates very easily at relatively low T_2 temperatures.

ZS samples. Section b of Fig. 4 shows that the catalytic activity of ZS samples is fairly low for activation at $T_2 \leq$ 773 K (see the curves relative to samples I and I*), whereas it increases for activation at $T_2 \geq$ 823 K. This observation is consistent with the findings of other researchers, for which good catalysts are obtained by sulfation of amor-

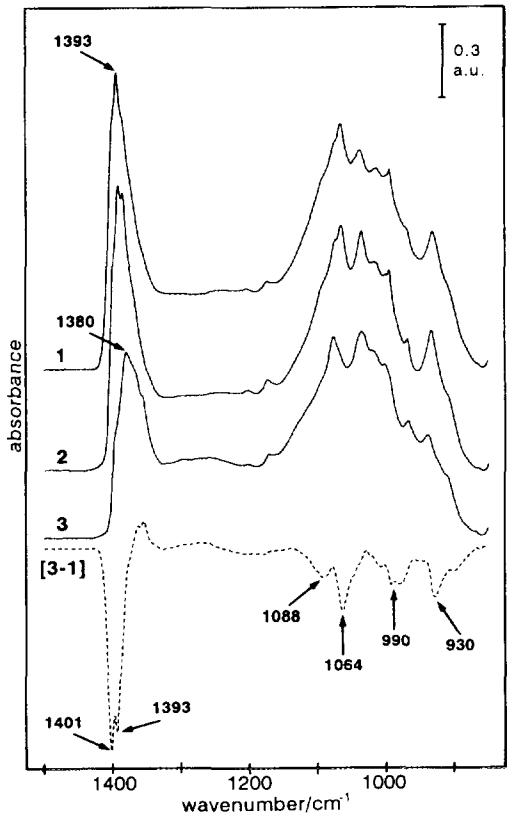

FIG. 5. Absorbance IR spectra in the ν(SO) vibrations region of some ZRP_{873} specimens. (1) ZRP_{873}[3.53H]673 (sample D); (2) ZRP_{873}[3.5H]773 (sample E); (3) ZRP_{873}[2.75H]923 (sample F); (broken trace [3 − 1]) the differential spectrum of samples F–D.

phous Zr hydrate, and also confirms the observation made by Sohn *et al.* (7) and Chen *et al.* (10) that catalyst activation at temperatures as high as 773–873 K is needed for the development of an appreciable catalytic activity.

It was suggested by the quoted authors that crystallization of the s.d.-ZrO_2 system must occur prior to the development of a catalytic activity, but the present data tend to contradict, at least in part, that hypothesis. In fact, with the present ZS samples, the onset of crystallization in the tetragonal ZrO_2 form occurs at temperatures definitely lower than those required for the onset of an appreciable catalytic activity; in particular, the difference of crystallinity exhibited by ZS samples calcined at 773 and 823 K (samples I* and J) is negligible, whereas the catalytic activity varies by a factor of $\approx$3.

It is so deduced that crystallization in the tetragonal form is, for s.d.-ZrO_2 systems, a necessary condition but not a sufficient condition for the development of catalytic activity in the isomerization of *n*-alkanes.

In addition, the overall concentration of surface sulfates, which has sometimes been invoked as an important parameter, does not seem to be primarily responsible for the observed evolution with T_2 of the catalytic activity of ZS samples. In fact, Table 1 shows that, on passing from T_2 = 673 K (sample I) to T_2 = 823 K (sample J), i.e., when the catalytic activity starts becoming high, the number of sulfate groups per unit area does indeed increase, as a consequence of the decrease of BET surface area and the residual water content. But, going from T_2 = 823 K (sample J) to T_2 = 923 K (sample K) the catalytic activity remains virtually constant in general terms or, if the decline in surface area is taken into account, increases further. In this temperature interval, the number of sulfates decreases appreciably, as a consequence of a partial sulfate decomposition faster than the decline in surface area, and consequently, the catalyst activity per mole SO_4 turns out to increase noticeably.

In the calcination temperature range in which the catalytic activity of ZS samples develops and grows, an important change in the spectral features of surface sulfates is observed (see Fig. 6). In fact:

(i) In the inactive sample calcined at T_2 = 673 (specimen I), the band of $\nu_{S=O}$ modes is centered at $\nu < 1400$ cm^{-1}, and the band of ν_{S-O} modes, centered at $\approx$1030 cm^{-1}, is broad, relatively weak, and ill-defined. Moreover, a strong broad and complex band is present in the 1250–1130 cm^{-1} interval. The latter band is thought to be due to the symmetric O=S=O vibrations (25) of surface sulfates

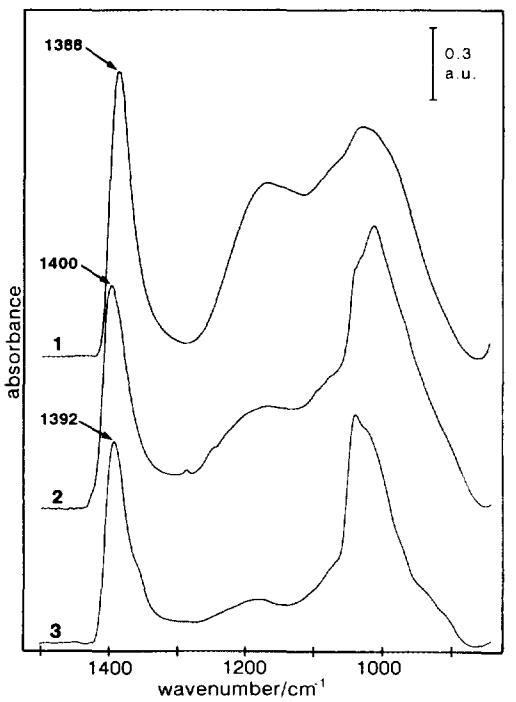

FIG. 6. Absorbance IR spectra in the ν(SO) vibrations region of some ZS specimens. (1) ZS[1.85N]673 (sample I); (2) ZS[2.6N]823 (sample J); (3) ZS[1.5N]923 (sample K).

carrying a SO_2 functionality in which the two coupled S=O oscillators form an angle different from 90°; the corresponding asymmetric stretching vibration modes would lie at higher frequencies, within the broad unresolved band centered at ≈1390 cm^{-1}.

It is thus inferred that surface sulfates, bound to the ZrO_2 network and structured so that the SO_2 functionality yields two coupled stretching vibrations (with a "regular" spectral separation of ≈250 cm^{-1} (21, 25)), are stable on tetragonal ZrO_2 materials that were calcined, after sulfation, at relatively low temperatures. Surface sulfates of this type turn out to be unable to induce in the zirconia system the superacid properties that lead to catalytic activity in the isomerization reaction of *n*-paraffins.

(ii) After calcination of the ZS samples at $T_2 > 773$ K (curves 2 and 3 of Fig. 6), the $\nu_{S=O}$ band maximum shifts to higher wavenumbers (≈1400 cm^{-1}), and the ν_{S-O} modes band assumes gradually the sharper and partly resolved aspect discussed in a previous section. Meanwhile, the broad band at 1250–1130 cm^{-1}, interpreted above as indicative of the presence of sulfates carrying vibrationally coupled S=O oscillators is gradually eliminated.

This transformation of the structure of surface sulfates, which initially occurs without any decline in the overall concentration of sulfates, leads the tetragonal ZrO_2 system to superacidity and to an appreciable catalytic activity in the isomerization reaction of *n*-alkanes.

The ZS sample calcined at $T_2 = 923$ K (specimen K, curve 3 of Fig. 6) is catalytically the most active; in it, surface sulfates with coupled S=O oscillators have been almost completely eliminated, whereas the surface sulfates characterized by a sharp $\nu_{S=O}$ band at a frequency slightly below 1400 cm^{-1} and by a sharp ν_{S-O} band at ≈1040 cm^{-1} are by far predominant. These are the SO vibrational modes that we have tentatively ascribed to covalent sulfates localized on crystallographic defects of the tetragonal ZrO_2 phase. These sulfate species, that we know from separate experiments to be thermally stable up to ≈1000 K, are thus thought to be mainly responsible for the superacid properties and catalytic activity of ZS specimens.

TO3 samples. Section c of Fig. 4 shows that the catalytic behaviour of the TO3 samples is fairly similar to that of the ZS samples dealt with in the previous section. In particular, only the TO3 catalysts calcined at $T_2 > 773$ K develop an appreciable catalytic activity, while the spectral features of surface sulfates undergo transformations similar to those described above for the ZS specimens, and for this reason are not shown in a figure. The importance of this observation is twofold.

(i) The tetragonal crystal phase of ZrO_2 is confirmed to be of primary importance (actually, it is a necessary condition) in determining the catalytic activity of a s.d.-ZrO_2 system, no matter what preparation route has been followed to obtain the tetragonal phase. This observation is in evident contradiction with what was reported by other authors (e.g., see Ref. (11)), who claim that sulfating crystalline ZrO_2 samples, both monoclinic *and* tetragonal, always leads to inactive systems. But the question is: after the sulfation step, was the tetragonal ZrO_2 solid used by these authors still tetragonal? In fact, our data presented in Figs. 1 and 2 show that, if the tetragonal ZrO_2 crystallites are not phase-stabilized (e.g., by the formation of a solid solution with Y_2O_3), the sulfation process tends to quantitatively transform the metastable tetragonal ZrO_2 phase into the stable monoclinic one. This phase transition is bound to lead to s.d.-ZrO_2 systems of virtually null catalytic activity.

(ii) The degree of crystalline order reached by the tetragonal ZrO_2 phase is *not* the determinant parameter that yields a good catalytic activity, as already postulated above with the ZS samples. In fact, Figs. 1 and 2 show that the increase in the calcination temperature to $T_2 = 923$ K does not modify appreciably the size of the crystallites nor the breadth of the XRD peaks of the TO3 samples. Also the surface area does not change much.

The structure of the family of covalent sulfate groups, which is characterized by two main strong absorptions at ≈1400 and ≈1030 cm^{-1} and which forms (only) at the surface of tetragonal ZrO_2 of any origin at $T_2 > 773$ K, so turns out to be the main parameter that determines superacid character and good catalytic activity in the s.d.-ZrO_2 systems.

CONCLUSIONS

Degree of crystallinity, crystallographic phase, sulfation procedure, and activation temperature of s.d.-ZrO_2 systems are (some out of many) preparative parameters, with a role in determining catalytic activity that has been mentioned in various instances. The role of these variables has never been systematically examined and has never been made clear. It is our opinion that the present results do throw some more light on the role they play.

(i) The sulfation process, almost independent of the sulfating agent, has almost no morphological or crystallographic effect on the monoclinic ZrO_2 phase. It converts the unstabilized tetragonal ZrO_2 phases into the monoclinic phase, still leaving the morphology of the crystallites virtually unchanged.

No appreciable morphological nor crystallographic effect is produced, by sulfation, on tetragonal ZrO_2 phases stabilized by the solid-solution with Y_2O_3.

As for amorphous (hydrated) ZrO_2 phases, the sulfation process leads to a morphological and structural evolution with temperature entirely different from that typical of nonsulfated systems. In fact, small crystallites and a pure

tetragonal ZrO_2 phase are favoured up to fairly high firing temperatures.

(ii) A stable tetragonal ZrO_2 phase is a necessary structural condition to obtain s.d.-ZrO_2 systems catalytically active in the isomerization reaction of *n*-alkanes. This condition is met either by sulfating an amorphous ZrO_2 precursor, as reported by other authors, or by sulfating a solid-solution stabilized crystalline *t*-ZrO_2 phase.

(iii) Thermal activation of tetragonal s.d.-ZrO_2 systems at temperatures $T_2 \geq \approx 800$ K is another necessary condition to obtain active s.d.-ZrO_2 catalysts, but this condition does not derive primarily from the degree of crystallinity.

Surface sulfates on active tetragonal s.d.-ZrO_2 catalysts are very different both from those prevailing on monoclinic s.d.-ZrO_2 systems and from those prevailing on inactive tetragonal s.d.-ZrO_2 ones activated at temperatures $T_2 < \approx 800$ K. The surface sulfates leading tetragonal s.d.-ZrO_2 systems to good catalytic activity in the isomerization of *n*-alkanes are characterized by (only) two strong broad bands due to ν(SO) vibrations, and are believed to correspond to

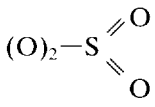

structures in which the two S=O oscillators form an angle close to 90°.

ACKNOWLEDGMENTS

This research was partly financed with funds of the CNR (Rome), Progetto Finalizzato Materiali Speciali. The preparation of TO3 samples and the recording of all XRD spectrograms were carried out by Dr. L. Montanaro and Dr. L. Ferroni of the Turin Polytechnic.

REFERENCES

1. Hino, H., and Arata, K., *J. Chem. Soc. Chem. Commun.*, 851 (1980).
2. Misono, M., and Okuhara, T., *Chemtech*, November, 23 (1993).
3. Umansky, B., Engelhardt, J., and Hall, W. K., *J. Catal.* **127,** 128 (1991).
4. Arata, K., *Adv. Catal.* **37,** 165 (1990).
5. Nascimento, P., Akratopoulou, C., Oszagyan, M., Coudurier, G., Travers, C., Joly, J. F., and Vedrine, J. C., *in* "Proceedings, 10th International Congress on Catalysis, Budapest, 1992" (F. Guczi, F. Solymosi, and P. Tétényi, Eds.), p. 1185, Akadémiai Kiadó, Budapest, 1993.
6. Morterra, C., Cerrato, G., Emanuel, C., and Bolis, V., *J. Catal.* **142,** 349 (1993).
7. Sohn, J. R., and Kim, H. W., *J. Mol. Catal.* **52,** 361 (1989).
8. Yamaguchi, T., *Appl. Catal.* **61,** 1 (1990).
9. Tanabe, K., Hattori, H., and Yamaguchi, T., *Crit. Rev. Surf. Chem.* **1,** 1 (1990).
10. Chen, F. R., Coudurier, G., Joly, J. F., and Vedrine, J. C., *J. Catal.* **143,** 616 (1993).
11. Comelli, R. A., Vera, C. R., and Parera, J. M., *J. Catal.* **151,** 96 (1995).
12. Morterra, C., Bolis, V., Cerrato, G., Pinna, F., Signoretto, M., and Strukul, G., *in* "Europacat-I, Montpellier Sept. 12–17, 1993," paper I-77, Vol. I, p. 150.
13. Morterra, C., Cerrato, G., Pinna, F., Signoretto, M., and Strukul, G., *J. Catal.* **149,** 181 (1994).
14. Pinna, F., Signoretto, M., Strukul, G., Cerrato, G., and Morterra, C., *Catal. Lett.* **26,** 339 (1994).
15. Bensitel, M., Saur, O., Lavalley, J. C., and Mabilon, G., *Mater. Chem. Phys.* **17,** 249 (1987).
16. Sarzanini, C., Sacchero, G., Pinna, F., Signoretto, M., Cerrato, G., and Morterra, C., *J. Mater. Chem.* **5**(2), 353 (1995).
17. Garvie, R. C., *J. Phys. Chem.* **69,** 1238 (1965); *J. Phys. Chem.* **82,** 218 (1985).
18. Morterra, C., Cerrato, G., Ferroni, L., and Montanaro, L., *Mater. Chem. Phys.* **37,** 243 (1994).
19. Evans, P. A., Stevens, R., and Binner, J. G. P., *Br. Ceram. Trans. J.* **83,** 39 (1984).
20. Bensitel, M., Saur, O., Lavalley, J. C., and Morrow, B. A., *Mater. Chem. Phys.* **19,** 147 (1988).
21. Bellamy, L. J., "The Infrared Spectra of Complex Molecules," Vol. I, 3rd ed., Chapman Hall, London, 1975.
22. Morterra, C., Bolis, V., Fubini, B., and Orio, L., *Surf. Sci.* **251/252,** 540 (1991).
23. Morterra, C., and Orio, L., *Mater. Chem. Phys.* **24,** 247 (1990).
24. Morterra, C., Cerrato, G., and Ferroni, L., *J. Chem. Soc. Faraday Trans.* **91**(1), 125 (1995).
25. Detoni, S., and Hadzi, D., *Spectrochim. Acta* **11,** 601 (1957).